Commun. Comput. Phys.
doi: 10.4208/cicp.080510.150511s

Vol. **11**, No. 4, pp. 1311-1322
April 2012

Statistics of Particle Suspensions in Turbulent Channel Flow

Lihao Zhao* and Helge I. Andersson

Fluids Engineering Division, Department of Energy and Process Engineering, Norwegian University of Science and Technology, 7491 Trondheim, Norway.

Received 15 May 2010; Accepted (in revised version) 15 May 2011

Available online 30 November 2011

Abstract. Particle dynamics in a turbulent channel flow is considered. The effects of particle concentration and Reynolds number on the particle velocity statistics are investigated. Four different particle response times, τ^+=1, 5, 30 and 100, are examined for three different Reynolds numbers, Re_*=200, 360 and 790 (based on channel height and friction velocity). The particle concentration evolves with time and statistics obtained during three different sampling periods might be distinctly different. The mean and fluctuating particle velocities are substantially affected both by the particle response time and by the Reynolds number of the flow.

AMS subject classifications: 76T15, 76F10, 76F65

Key words: Spherical particles, DNS, turbulence, sampling, Reynolds number effects.

1 Introduction

Solid spherical particles suspended in fluid turbulence are commonly encountered both in nature and industry, e.g. in sand storms, pollution in the atmosphere, in pneumatic transport and so on. The study of particles suspended in a carrier fluid has been an active area of research during several decades along with the development of computer resources and experiment technologies [1,2]. It is commonly known that inertial particles will not follow the flow totally passive. Due to the inertial effect, there is a certain amount of slip velocity between particles and the local fluid flow. In other words, the inertial solid particles have a tendency to concentrate around locally calm regions [1]. In the channel flow case, for example, the particles tend to accumulate in the near-wall region and the greater the inertia of particles, the longer time is needed to achieve a steady state of the particle concentration. Several investigations have focused on the particle deposition and

*Corresponding author. *Email addresses:* lihao.zhao@ntnu.no (L. H. Zhao), helge.i.andersson@ntnu.no (H. I. Andersson)

particle preferential concentration in wall turbulence or homogenous turbulence, see for instance Pedinotti *et al*. [2], Soltani and Ahmadi [3], Marchioli and Soldati [4], Narayanan *et al*. [5] and Picciotto *et al*. [6]. To obtain better understanding of particle transport and particle velocity statistics, several studies were reported by Marchioli and Soldati [4], Kulick *et al*. [7]. and Geashchenko *et al*. [8].

Depending on the particle volume fraction, there are several ways to make the coupling between the particle phase and the fluid phase, i.e. as one-way, two-way or four-way coupling, as defined by Elghobashi [9]. With *one-way* coupling, e.g. [4, 6], the particles are driven by the local flow, but there is no feedback effect from particles on the fluid. This approach is suitable for sufficiently dilute suspension flows when the particle volume fraction is small. *Two-way* coupling means interactions between the particle phase and the fluid phase based on Newtons third law, while *four-way* coupling not only considers the interaction between particles and fluid, but also includes the effect of inter-collisions among the particles themselves. Several investigations with two-way coupling, like Squires and Eaton [10] and Elgobashi and Truesdell [11] in homogeneous turbulence, Pan and Banerjee [12] and Zhao *et al*. [13] in wall-bounded turbulence, focus on the modulations of turbulence by the presence of particles. The present work is confined to one-way coupling as we assume a dilute suspension of the particles in the carrier fluid and focuses on the Reynolds number effect on the particle transport and particle depositions.

During the last two decades direct numerical simulations (DNSs) have become a powerful tool in the research of turbulent flow of particle suspensions, for example DNS simulations of particle-laden homogeneous and isotropic turbulence [10, 11] and also of particulate turbulent channel flow [2–4, 12, 13]. However, all these simulations were carried out at fairly low Reynolds numbers, most likely due to limitations of the available computer capacity.

In the present investigation a dilute suspension of solid particles in a turbulent channel flow is simulated with an Eulerian-Lagrangian approach where the fluid flow is obtained by means of DNS. In Section 2, the treatment of the flow and the particles is described. Results for four different particle categories are presented and compared in Section 3.1 for one particular Reynolds number whereas results for three different Reynolds numbers are presented in Section 3.3. The highest Reynolds number considered is substantially higher than in earlier DNS studies of particle-laden channel flows [2–6, 12, 13]. The major findings are discussed and summarized in Section 4, notably in view of the influence of the particle concentration on the velocity statistics.

2 Mathematical modeling and computational details

In the present work we consider the motion of tiny spherical particles in a turbulent plane channel flow. The equations governing the flow field and particle motion are simultaneously integrated forward in time. The flow solver and the particle treatment is the same as that used by Mortensen *et al*. [14, 15].

2.1 Governing equations of the fluid flow

DNS is used to solve the continuity and momentum conservation equations:

$$\nabla\cdot\vec{u}=0, \tag{2.1}$$

$$\frac{\partial\vec{u}}{\partial t}+(\vec{u}\cdot\nabla)\vec{u}=-\nabla p+\frac{\nabla^2\vec{u}}{Re_*} \tag{2.2}$$

for an isothermal and incompressible Newtonian fluid. Here, $\vec{u}$ and p are the instantaneous velocity vector and pressure and ∇ is the gradient operator. The flow field is determined by the friction Reynolds number $Re_*=hu_*/\nu$ based on the wall distance h, the friction velocity u_* and the kinematic viscosity ν of the fluid. The flow is driven by a constant pressure gradient in the streamwise direction in order to overcome the wall friction. Here, simulations will be performed at three different Reynolds numbers 200, 360 and 790 from which some primary statistics will be compared.

The size of the computational domain is the same as in [14] and [15], namely a length $6h$ in the streamwise x-direction and a width $3h$ in the spanwise y-direction. Periodic boundary conditions are imposed in the homogeneous x- and y-directions and no-slip and impermeability were enforced at the solid walls at $z=0$ and $z=h$. A mesh with 192*192*192 grid points is used for the two lower Reynolds numbers and a finer mesh with 384*384*384 grid points is used for $Re_*=790$. The mesh sizes in wall units ν/u_* thus become $\triangle x^+=2\triangle y^+=6.25$ (11.25) and the grid spacing $\triangle z^+$ in the wall-normal direction varies from 0.49 to 1.59 $(0.88-2.86)$ for $Re_*=200$. The values in the parenthesis refer to the intermediate Reynolds number 360. The resolution for the highest Reynolds number is comparable with that for $Re_*=360$.

The same numerical scheme as that used by Mortensen *et al*. [14, 15] and Gillissen *et al*. [16] is employed in the present study to integrate the Eulerian flow equations (2.1)-(2.2). This is based on a pseudo-spectral method in which the spatial derivatives in the two homogeneous directions are obtained in spectral space by means of Fourier-series representations. A second-order accurate finite-difference scheme on a staggered grid system is used for the derivatives in the wall-normal direction. The time advancement is carried out with a second-order explicit Adams-Bashforth scheme. Mass conservation is assured by means of a standard projection method and the resulting Poisson equation is transformed to Fourier space in the homogeneous directions.

2.2 Governing equations for the particle motion

The translational motions of the particles are computed from Newton's second law, i.e. in a Lagrangian approach. Only the Stokes drag is considered in present work, while other forces, such as lift and virtual mass forces, are neglected. The particle Reynolds number Re_p should be smaller than unity in order to satisfy the assumption of Stokes flow in the immediate vicinity of a particle. The size of the particles is smaller than smallest eddies in

the flow such that the force on the particle can be treated as a point force. The governing equation of particle motion then becomes:

$$\frac{d\vec{v}}{dt}=\frac{1}{\tau}(\vec{u}(x_p,t)-\vec{v}). \tag{2.3}$$

In Eq. (2.3), v is the translational velocity of the particle and u is the velocity of fluid at the location x_p of the particle. τ is the *particle response time* defined as:

$$\tau=\frac{2Sa^2}{9\nu},\qquad \tau^+=\tau\frac{u_*^2}{\nu}. \tag{2.4}$$

Here, S is the density ratio between particle and fluid, and a is the radius of the particle. τ^+ denotes the particle response time normalized by the viscous time scale ν/u_*^2. In order to determine the slip velocity which determines the Stokes drag in Eq. (2.3), the fluid velocity $u(x_p,t)$ at the particle position x_p is interpolated from the staggered grid on which the fluid motion is obtained onto the particle position. The interpolation scheme used is quadratic and involves the 27 closest grid points.

The particles are initially distributed randomly throughout the already fully developed turbulent flow field. The particle velocity is initially set equal to the local fluid velocity. The governing equation of particle motion (2.3) is integrated in time with a second-order accurate Adams-Bashforth scheme. The time-step used in this integration is the same as the time-step used for the integration of Navier-Stokes equation (2.2), which is sufficiently smaller than the particle response time.

3 Results

The present approach is based on the assumption that the particle suspension is sufficiently dilute and that the size of the particles is smaller than the Kolmogorov length scale. Based on these assumptions, the simulations are one-way coupled, which means that the particles are affected by the fluid but there is no feedback from the particles onto the flow. The flow field is obtained by means of DNS for the three different frictional Reynolds numbers 200, 360, and 790. The four different particle response times $\tau^+=1$, 5, 30, and 100 (see Table 1) are considered at all the three Reynolds numbers. The same number of particles N_p is used in all the 12 simulations. At the low and intermediate Re_* an almost steady particle concentration distribution is reached during the course of the simulations.

3.1 Choice of sampling period $-Re_*=200$

The initiation of statistics sampling and the duration T of the sampling period are believed to have a crucial impact on the particle statistics. Due to particle inertia, the majority of the particles tend to distribute inside of the viscous sublayer and the number

Table 1: Particle properties. The same four particle cases are considered for all three Reynolds numbers. The superscript $+$ refers to normalization with viscous units.

Case	τ^+	a^+	S	N_p
A	1	0.36	34.7	10^5
B	5	0.36	173.6	10^5
C	30	0.36	1041.7	10^5
D	100	0.36	3472.2	10^5

of particles in the center part of the channel is accordingly reduced. This phenomenon can affect the quality of the sampled data and different sampling periods may give rise to different statistical results. The time development of number of particles in the region $z^+ < 12$ is shown in Fig. 1 for $Re_* = 200$. This means that we are counting only the particles in the innermost near-wall region, i.e. inside of where the turbulent kinetic energy reaches its peak level. Three different sampling periods are considered, each of length $T^+ = 2820$. During a sampling period 141 samples are taken, equally separated in time. The sampling periods labeled 1, 2, and 3 in Fig. 1 are in an early stage of the simulation, at an intermediate state, and at an almost statistically steady state, respectively.

Primary particle velocity statistics for $\tau^+ = 5$ and $\tau^+ = 30$ are shown in Fig. 2 and Fig. 3, respectively. The results obtained during Sampling 2 and Sampling 3 (see Fig. 1) are almost indistinguishable. This observation implies that reliable sampling can be performed although the particle concentration still changes with time. However, if the sampling is done at a too early stage of the simulation, i.e. Sampling 1, the resulting statistics deviate

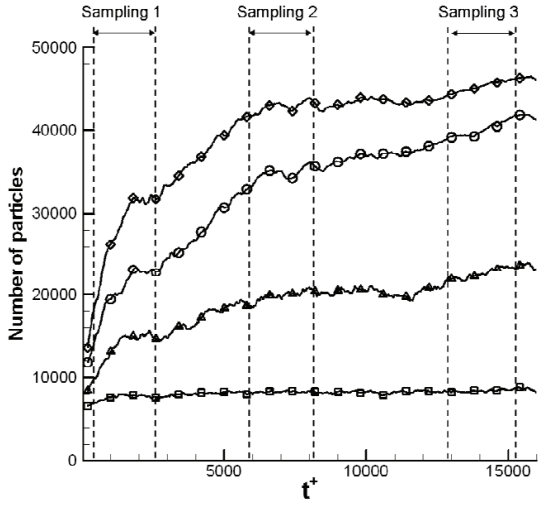

Figure 1: Development of particle concentration in the near-wall region $z^+ < 12$ for $Re_* = 200$. The double arrows show three different sampling periods each of duration 2820 viscous time units. $\tau^+ = 1$, squares; $\tau^+ = 5$, triangles; $\tau^+ = 30$, diamonds; $\tau^+ = 100$, circles.

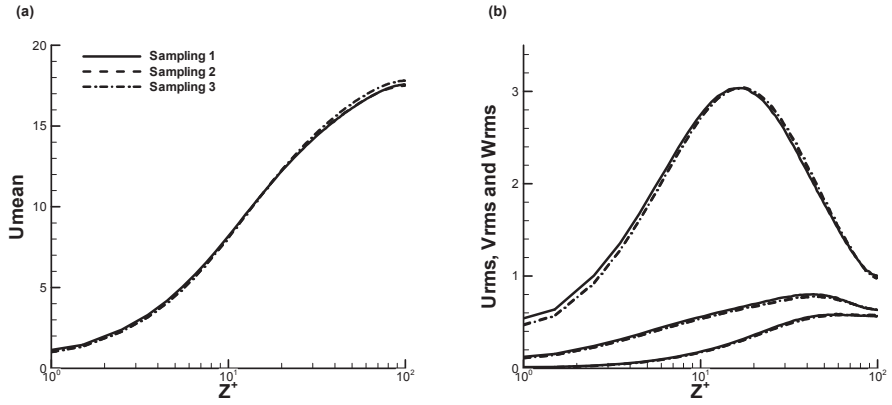

Figure 2: Streamwise mean particle velocity (a) and RMS velocity fluctuations (b) for $\tau^+=5$.

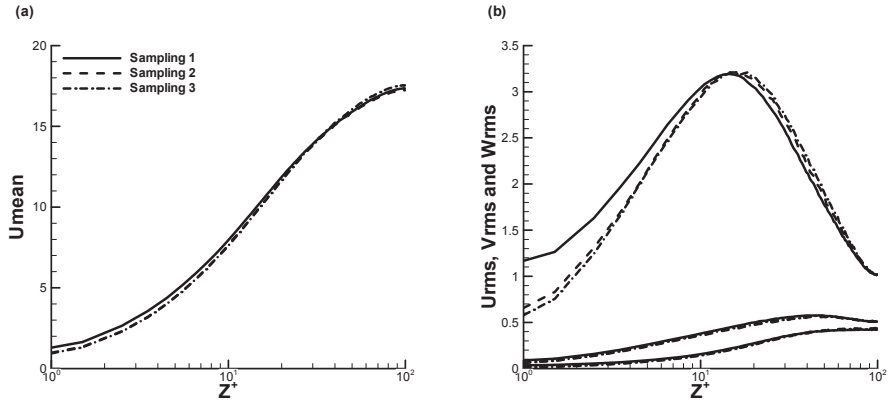

Figure 3: Streamwise mean particle velocity (a) and RMS velocity fluctuations (b) for $\tau^+=30$.

from those obtained later on. This tendency is observed in the near-wall region for the $\tau^+=5$ particles in Fig. 2, but the effect is more pronounced for the slower particles in Fig. 3. A longer time is required for the $\tau^+=30$ particles to adapt to the local flow conditions in the viscous sub-layer. These findings are consistent with the recommendation made by Zhang *et al*. [17] that sampling should be performed under quasi-equilibrium conditions when the particle mass flux towards the wall has become almost constant. The above results demonstrate that not only the length of the sampling period matters. The start of the sampling is also of major concern to ensure reliable particle statistics.

3.2 Verification of the high-Reynolds-number case $-Re_*=790$

The vast majority of DNSs of dilute particle suspensions are performed at fairly low Reynolds numbers; see e.g. Marchioli *et al*. [18] where the benchmarking were performed at Reynolds number $Re_*=300$. In order to investigate the Reynolds number effect on the

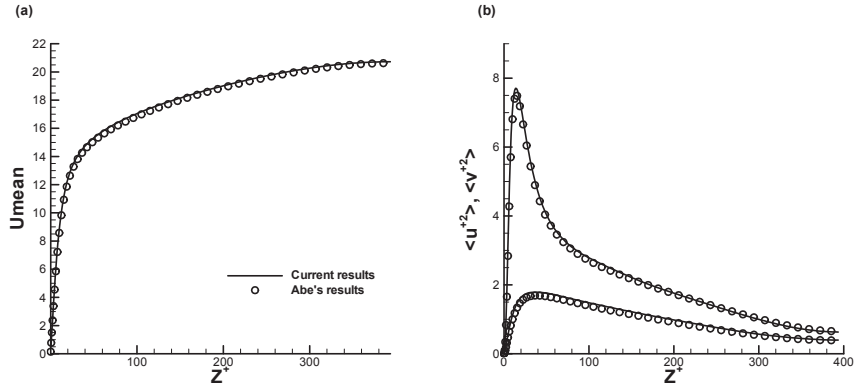

Figure 4: Mean streamwise fluid velocity (a) and velocity fluctuations $<u^{+2}>$, $<v^{+2}>$ (b). Results from the present simulation at $Re_*=790$ (lines) are compared with DNS data from Abe et al. [19, 20] at the same Reynolds number.

particle dynamics, we also performed simulations at higher *Re*. In order to verify that the turbulent channel flow field is realistic, the mean fluid velocity and the streamwise and spanwise velocity variances $<u^{+2}>$ and $<v^{+2}>$ are compared with DNS data from Abe *et al*. [19] at the same Reynolds number. Their data is available at the database [20]. The comparisons in Fig. 4 show an almost perfect agreement between the present results and those of Abe *et al*. [19, 20].

3.3 Reynolds number effects

Results for the three different Reynolds numbers considered will now be examined. First of all, let us recall that the variance of the fluid velocity components increases with increasing Reynolds number, in keeping with the earlier findings of Abe *et al*. [19] and others, see e.g. Fig. 5 in which results for the fastest particles ($\tau^+=1$) are presented. It is noteworthy that the fluid and particle velocities coincide in almost all respects, except when the streamwise velocity fluctuations are considered in Fig. 5(b). These fast particles behave almost as passive tracer particles. The modest deviation between particle and fluid streamwise velocities is due to preferential concentration of the particles in the near-wall region, see e.g. Eaton & Fessler [1] and Marchioli & Soldati [4]. Near-wall regions with locally low streamwise fluid velocity are left almost empty of particles.

Particle velocity statistics for the slower (or heavier) particles with response times $\tau^+=5$, 30 and 100 are shown in Figures 6 - 8, respectively. Notice that the fluid velocity statistics are the same throughout since the particles do not affect the flow field in the one-way coupled simulations. The mean particle velocity coincides with the mean fluid velocity, except for $\tau^+=30$ particles at $Re_*=200$ in Fig. 7(a) and for the slowest (heaviest) particles in Fig. 8(a). The deviation between mean particle and fluid velocities is most pronounced at the lowest Reynolds number and becomes almost negligible in the high-*Re* case in Fig. 8(a).

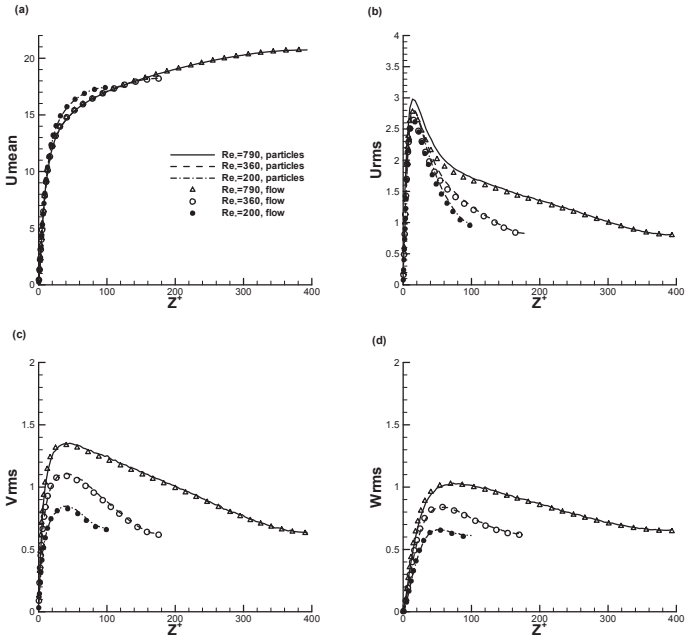

Figure 5: Comparison between fluid and particle mean velocity (a) and velocity fluctuations in the streamwise (b), spanwise (c), and wall-normal (d) directions for $\tau^+=1$. The symbols denote fluid velocities and the lines represent particle velocities. The profiles are terminated at the mid-plane of the channel.

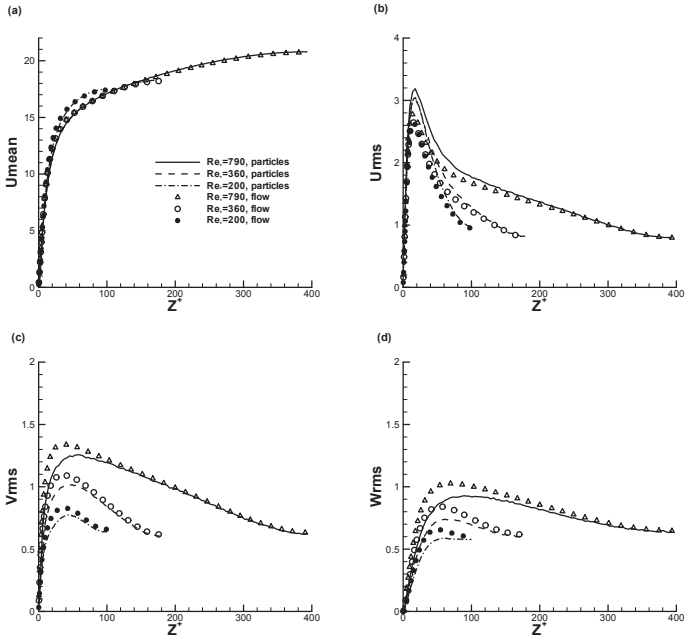

Figure 6: Comparison between fluid and particle mean velocity (a) and velocity fluctuations in the streamwise (b), spanwise (c), and wall-normal (d) directions for $\tau^+=5$. The symbols denote fluid velocities and the lines represent particle velocities. The profiles are terminated at the mid-plane of the channel.

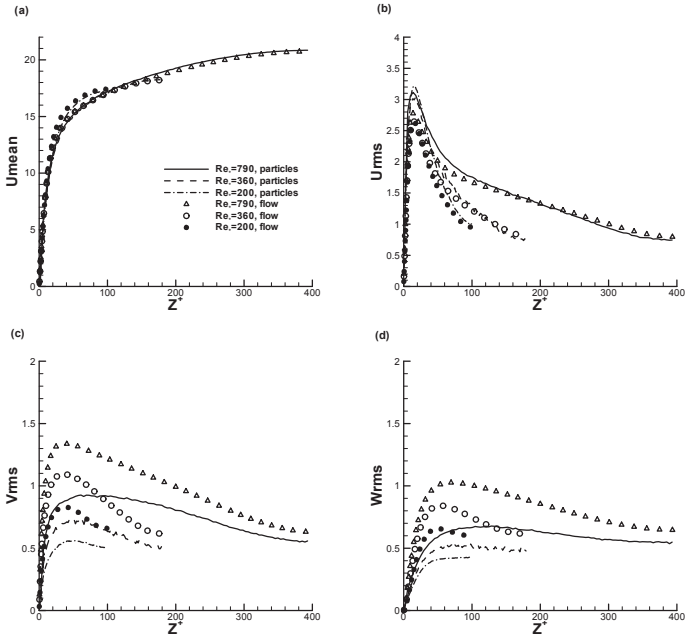

Figure 7: Comparison between fluid and particle mean velocity (a) and velocity fluctuations in the streamwise (b), spanwise (c), and wall-normal (d) directions for $\tau^+=30$. The symbols denote fluid velocities and the lines represent particle velocities. The profiles are terminated at the mid-plane of the channel.

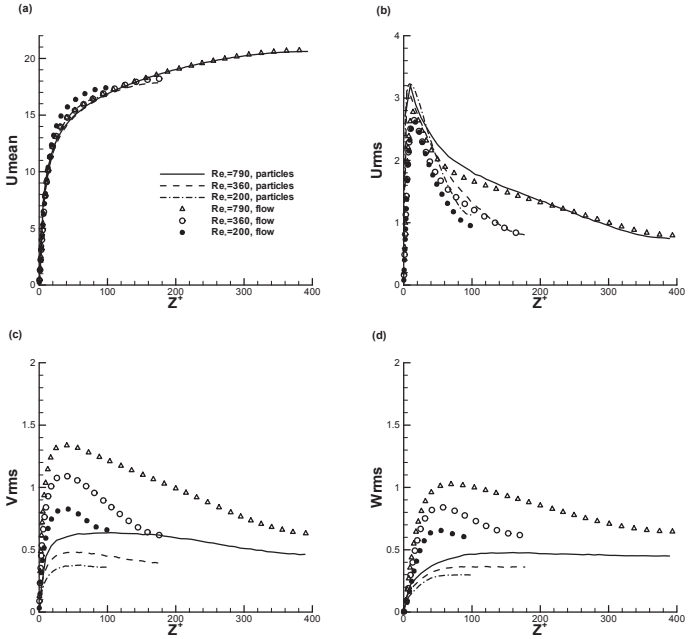

Figure 8: Comparison between fluid and particle mean velocity (a) and velocity fluctuations in the streamwise (b), spanwise (c), and wall-normal (d) directions for $\tau^+=100$. The symbols denote fluid velocities and the lines represent particle velocities. The profiles are terminated at the mid-plane of the channel.

The particle velocity fluctuations in the streamwise direction are distinctly different from the fluid velocity fluctuations already for τ^+=5 particles, as shown in Fig. 5(b), whereas the spanwise and wall-normal fluctuations in Fig. 5(c)-(d) are almost the same for the particle and the fluid. However, substantial differences are observed in all three directions for the slower particles. In spite of the large differences between fluid and particle velocity fluctuations, the latter show the same increasing trend with *Re* as the fluid velocity fluctuations.

4 Discussion and concluding remarks

The objective of the present investigation has been to compare particle statistics in turbulent channel flow at three different Reynolds numbers and for particles with four different relaxation times ranging from fast ($\tau^+ = 1$) to slow ($\tau^+ = 100$). Since almost all earlier DNS studies on particle dynamics in turbulent shear flows have been carried out at fairly low Reynolds numbers (e.g. at $Re_* = 300$ in [4, 18] and at $Re_* = 360$ in [14, 15]), an examination of Reynolds number effects was considered timely. First, however, we considered some different choices of the sampling period during which statistics were gathered. It was demonstrated that it is not required to postpone the sampling until the particle concentration has reached a steady state. On the contrary, a too early sampling may lead to misleading statistics.

A major observation regarding the particle velocity fluctuations is the pronounced increase at higher Reynolds numbers. This is fully consistent with the well-known Reynolds number effect on the fluid velocity fluctuations, see e.g. Abe *et al*. [19]. This effect is most prominent for the spanwise (v′) and wall-normal (w′) fluctuations. The streamwise particle velocity fluctuations u′, on the other hand, exhibit no distinct Reynolds number effect for the slowest particles in Fig. 8(b). It is also noteworthy that in spite of the increasing trend of v′ and w′ with *Re*, the *shape* of the intensity profiles in Fig. 8 is rather different from those of the fluid intensity profiles. The near-wall peaks of the turbulence intensity distributions are almost absent in the particle intensity profiles. This is probably due to the preferential particle clustering in near-wall areas where the fluid motion is predominantly in the streamwise direction.

It is generally observed that the differences between the particle and fluid velocities increase with increasing response times, i.e. for slower and/or heavier particles. Let us therefore recall that the present simulations were one-way coupled. The deviation between particle and fluid velocities will undoubtedly be altered in a two-way coupled simulation. Intuitively two-way coupling will tend to reduce the deviation between fluid and particle velocities, but the amount of adaption will obviously depend on the particle response time. The present data are nevertheless believed to exhibit the same qualitative features as more realistic two-way coupled simulations.

From the present data, we observed that the particles fluctuated less vigorously than the fluid in the spanwise wall-normal directions, whereas the streamwise agitation of

the particles exceeded the streamwise turbulence intensity (see e.g. Figs 7 and 8). We will therefore conjecture that the presence of the particles in a two-way coupled simulation will tend to enhance the streamwise fluid velocity fluctuations and correspondingly reduce the spanwise and wall-normal fluctuations. This happens to be the signature of drag reduction achieved by polymers, as reviewed recently by Graham [21]. We are therefore inclined to speculate, on the basis of the present results, that drag reduction can be archived also by means of solid spherical particles. This conjecture was in fact approved while the present manuscript was being reviewed. Two-way coupled simulations with τ^+=30 particles at a friction Reynolds number Re_*=360 reported by Zhao *et al*. [13] exhibited the anticipated modulation of the turbulent flow field which resulted in a significant drag reduction.

Acknowledgments

This article is a slightly expanded version of a paper with the same title presented by the first author at "The 8^{th} Asian Computational Fluid Dynamics Conference" in Hong Kong $10^{th}-14^{th}$ January 2010. The research work reported herein has been supported by A/S Norske Shell through a research fellowship (contract No. 4610020178/C08156) and by the Research Council of Norway (Programme for Supercomputing) through a grant of computing time.

References

[1] J. K. Eaton and J. R. Fessler, Preferential concentration of particles by turbulence. Int. J. Multiphase Flow, 20 (1994), 169-209.
[2] S. Pedinotti, G. Mariotti and S. Banerjee, Direct numerical simulation of particle behaviour in the wall region of turbulent flows in horizontal channels. Intl J. Multiphase Flow, 18 (1992), 927-941.
[3] M. Soltani and G. Ahmadi, Direct numerical simulation of particle entrainment in turbulent channel flow. Phys. Fluids, 7 (1995), 647-657.
[4] C. Marchioli and A. Soldati, Mechanisms for particle transfer and segregation in a turbulent boundary layer. J. Fluid Mech., 468 (2002), 283-315.
[5] C. Narayanan, D. Lakehal, L. Botto and A. Soldati, Mechanisms of particle deposition in a fully developed turbulent open channel flow. Phys. Fluids, 15 (2003), 763-775.
[6] M. Picciotto, C. Marchioli and A. Soldati, Characterization of near-wall accumulation regions for inertial particles in turbulent boundary layers. Phys. Fluids, 17 (2005), 098101.
[7] J. D. Kulick, J. R. Fessler and J. K. Eaton, Particle response and turbulence modification in fully developed channel flow. J. Fluid Mech., 227 (1994), 109-134.
[8] S. Geashchenko, N. Sharp, S. Neuscamman and Z. Warhaft, Lagrangian measurements of inertial particle accelerations in a turbulent boundary layer. J. Fluid Mech., 617 (2008), 255-281.
[9] E. Elghobashi, On predicting particle-laden turbulent flows. Appl. Sci. Res., 52 (1994), 309-329.

[10] K. D. Squires and J. K. Eaton, Particle response and turbulence modification in isotropic turbulence. Phys. Fluids A, 2 (1990), 1191-1203.
[11] S. Elghobashi and G. C. Truesdell, On the two-way interaction between homogeneous turbulence and dispersed solid particles. I: Turbulence modification. Phys. Fluids A, 5 (1993), 1790-1801.
[12] Y. Pan and S. Banerjee, Numerical simulation of particle interactions with wall turbulence. Phys. Fluids, 8 (1996), 2733-2755.
[13] L. H. Zhao, H. I. Andersson and J. J. J. Gillissen, Turbulence modulation and drag reduction by spherical particles. Phys. Fluids, 22 (2010), 081702.
[14] P. H. Mortensen, H. I. Andersson, J. J. J. Gillissen and B. J. Boersma, Statistics of dilute particle suspensions in wall-bounded turbulence. Proc. 4^{th} National Conference on Computational Mechanics, Tapir Academic Press (2007), 259-271.
[15] P. H. Mortensen, H. I. Andersson, J. J. J. Gillissen and B. J. Boersma, Particle spin in a turbulent shear flow. Phys. Fluids, 19 (2007), 078109.
[16] J. J. J. Gillissen, B. J. Boersma, P. H. Mortensen and H. I. Andersson, On the performance of the moment approximation for the numerical computation of fibre stress in turbulent channel flow. Phys. Fluids, 19 (2007), 035102.
[17] H. Zhang, G. Ahmadi, F.-G. Fan and J. B. McLaughlin, Ellipsoidal particles transport and deposition in turbulent channel flows. Int. J. Multiphase Flow, 27 (2001), 971-1009.
[18] C. Marchioli, A. Soldati, J. G. M. Kuerten, B. Arcen, A. Tanière, G. Goldensoph, K.D. Squires, M. F. Cargnelutti and L.M. Portela, Statistics of particle dispersion in direct numerical simulations of wall-bounded turbulence: Results of an international collaborative benchmark test. Int. J. Multiphase Flow, 34 (2008), 879-893.
[19] H. Abe, H. Kawamura, H. Choi, Very large-scale structures and their effects on the wall shear-stress fluctuations in turbulent channel flow up to $Re_\tau = 640$. J. Fluids Eng., 126 (2004), 835-843.
[20] Database `http://murasun.me.noda.tus.ac.jp`.
[21] M. D. Graham, Drag reduction in turbulent flow of polymer solutions. Rheology Reviews, (2004), 143-170.